# Retinal Manifestations of Mitochondrial Oxidative Phosphorylation Disorders

Jin Kyun Oh,[1,2] Jose Ronaldo Lima de Carvalho Jr,[1,3,4] Yan Nuzbrokh,[1,5] Joseph Ryu,[1] Teja Chemudupati,[6] Vinit B. Mahajan,[6,7] Janet R. Sparrow,[1,8] and Stephen H. Tsang[1,8]

[1]Jonas Children's Vision Care, Department of Ophthalmology, Columbia University Irving Medical Center, New York, New York, United States
[2]State University of New York at Downstate Medical Center, Brooklyn, New York, United States
[3]Department of Ophthalmology, Empresa Brasileira de Servicos Hospitalares (EBSERH) - Hospital das Clinicas de Pernambuco (HCPE), Federal University of Pernambuco (UFPE), Recife, Pernambuco, Brazil
[4]Department of Ophthalmology, Federal University of São Paulo (UNIFESP), São Paulo, São Paulo, Brazil
[5]Renaissance School of Medicine at Stony Brook University, Stony Brook, New York, United States
[6]Molecular Surgery Laboratory, Byers Eye Institute, Stanford University, Palo Alto, California, United States
[7]Veterans Affairs Palo Alto Health Care System, Palo Alto, California, United States
[8]Department of Pathology and Cell Biology and Columbia Stem Cell Initiative (CSCI), Columbia University Irving Medical Center, New York, New York, United States

**PURPOSE.** The purpose of this paper was to discuss manifestations of primary mitochondrial dysfunctions and whether the retinal pigment epithelium or the photoreceptors are preferentially affected.

**METHODS.** A retrospective analysis was performed of patients with clinically and laboratory confirmed diagnoses of maternally inherited diabetes and deafness (MIDD) or Kearns–Sayre syndrome (KSS). Patients underwent full ophthalmic examination, full-field electroretinogram, and multimodal imaging studies, including short-wavelength autofluorescence, spectral domain-optical coherence tomography, and color fundus photography.

**RESULTS.** A total of five patients with MIDD and four patients with KSS were evaluated at two tertiary referral centers. Mean age at initial evaluation was 50.3 years old. Nascent outer retinal tubulations corresponding with faint foci of autofluorescence were observed in two patients with MIDD. Characteristic features of this cohort included a foveal sparing phenotype observed in 13 of 18 eyes (72%), global absence of intraretinal pigment migration, and preserved retinal function on full-field electroretinogram testing in 12 of 16 eyes (75%). One patient diagnosed with MIDD presented with an unusual pattern of atrophy surrounding the parapapillary region and one patient with KSS presented with an atypical choroideremia-like phenotype.

**CONCLUSIONS.** MIDD and KSS are phenotypically heterogeneous disorders. Several features of disease suggest that primary mitochondrial dysfunction may first affect the retinal pigment epithelium followed by secondary photoreceptor loss. Similarities between primary mitochondrial degenerations and retinal disorders, such as age-related macular degeneration may suggest a primary role of mitochondria in the pathogenesis of these oligogenic disorders.

Keywords: mitochondria, retinal pigment epithelium, inherited retinal degeneration

The pivotal role of mitochondria in the metabolic ecosystem of the retina has been a subject of interest in understanding the pathophysiology of several forms of retinal degeneration.[1] In the healthy retina, a codependence exists between the retinal pigment epithelium (RPE) and photoreceptors, as both rely on the other to satisfy their energy requirements.[2–5] Photoreceptors derive energy from anaerobic glycolysis, using glucose transported from the choroid by the RPE, to produce adenosine triphosphate (ATP) and lactate.[2–7] In contrast, the RPE produces ATP from oxidative phosphorylation along the inner membrane of mitochondria

using substrates, such as lactate produced by the photoreceptors, lipids, and ketone bodies.[2–5]

Disruption of these interdependent processes has been suggested to cause dysfunction of both the RPE and photoreceptors, leading to several degenerative retinal disorders. In conjunction with the described metabolic coupling system, we hypothesize that dysfunction of the mitochondria in the RPE in many of these disorders renders the RPE cells unable to produce ATP through oxidative phosphorylation, requiring that primary production of energy occurs through glycolysis.[8] This, in turn, deprives the photoreceptors of glucose

from the choroid and leads to a decrease in production of lactate and other intermediates that can be used by the remaining functional mitochondria in the RPE, leading to a continuing cycle ending with cell death.[1,8–14] Primary mitochondrial disorders of the retina are those in which the first pathogenic event is the inheritance or development of a mutation within the mitochondrial genome. These conditions include maternally inherited diabetes and deafness (MIDD), which may present as a pattern macular dystrophy, and Kearns-Sayre syndrome (KSS), which can present with pigmentary retinal changes.

Evaluation of these primary mitochondrial retinal disorders may help not only improve our understanding of disease pathophysiology, but also elucidate the mechanisms that govern other complex retinal diseases, such as age-related macular degeneration (AMD). AMD is a multifactorial disease with numerous genomewide associations, including those related to immune function, lipid metabolism, and the extracellular matrix.[15,16] Among these pathways, several studies have suggested that the mitochondria within the RPE are an important site of disease pathogenesis.[1,8–14] A histopathologic study of eyes donated from patients with AMD demonstrated a significant reduction in mitochondria numbers and disruption of the mitochondrial cristae within the RPE.[9,11] A genetic analysis of eyes donated from patients with AMD revealed a significant correlation between carriers of the high-risk allele for *CFH*, a complement associated gene, and higher levels of mitochondrial DNA (mtDNA) damage.[17] Although additional study is warranted to identify the mechanism by which mtDNA damage influences AMD pathogenesis and what other known risk alleles for AMD may be associated with increased mtDNA damage, these findings suggest that mitochondria play an important role in AMD.

In this study, we compare and discuss a series of five patients diagnosed with MIDD and four patients diagnosed with KSS, all of whom had phenotypically variable retinal degeneration. Several features of this cohort may suggest that primary mitochondrial dysfunction may lead to primary degeneration of RPE followed by secondary photoreceptor loss.

## METHODS

### Subjects

Retrospective analysis of nine unrelated patients (P1–P9) with diagnoses of MIDD or KSS was performed. All patients were evaluated at the Edward S. Harkness Eye Institute at Columbia University Irving Medical Center and the Byers Eye Institute at Stanford University School of Medicine. Informed consent was waived due to the retrospective nature of the study design and the minimal risk conferred to patients. This study was performed under Columbia University Institutional Review Board-approved protocol AAAR8743 and Stanford University Institutional Review Board-approved protocol 42754. All procedures were in accordance with the tenets of the Declaration of Helsinki.

### Ophthalmic Examination

Patients underwent full ophthalmic examination, including measurement of best-corrected visual acuity followed by dilation with tropicamide (1%) and phenylephrine (2.5%), fundus examination, and multimodal imaging. Multimodal

imaging included spectral domain optical coherence tomography (SD-OCT), short-wavelength fundus autofluorescence (SW-AF, 488 nm excitation), and color fundus photography. SD-OCT scans were acquired on a Spectralis HRA + OCT (Heidelberg Engineering, Heidelberg, Germany). SW-AF images were obtained in 30 degree × 30 degree field using a Spectralis HRA + OCT or in a wide field image using an Optos 200 Tx (Optos, PLC, Dunfermline, UK) that was subsequently cropped to a 30 degree × 30 degree field. Wide field color fundus photographs were obtained using an Optos 200 Tx (Optos, PLC).

### Full-Field Electroretinogram

Full-field electroretinography (ffERG) was performed using Dawson, Trick, and Litzkow (DTL) electrodes and Ganzfeld stimulation according to international standards.[18] A Diagnosys Espion Electrophysiology System (Diagnosys LLC, Littleton, MA, USA) was used to obtain the ffERG.

### Mitochondrial Testing

The mtDNA was isolated and analyzed from peripheral blood, urine, or muscle biopsy in all patients. Five samples underwent sequencing of the whole mtDNA on Illumina MiSeq technology and were compared to a reference mtDNA sequence (RCRS). Two samples were analyzed using long range polymerase chain reaction amplification and massive parallel sequence analysis. Two samples were analyzed using a Southern blot for mitochondrial deletions following DNA digestion with PvuII restriction endonuclease.

## RESULTS

### Clinical Summary

The clinical and demographic information for all nine patients is summarized in Table 1. Five patients (P1–P5) were diagnosed with MIDD whereas four patients (P6–P9) were diagnosed with KSS. The mean and median age of visual symptom onset were 35 and 31 years old and the mean and median age at initial evaluation were 50.3 and 57 years old.

Four of the five patients diagnosed with MIDD had symptoms of nyctalopia (P4), central vision loss (P3), or both (P1 and P5). P2 presented with a history of floaters. Three of the five patients with MIDD (P1, P2, and P5) had hearing loss. P5 had a diagnosis of type I diabetes mellitus (T1DM) as well as a family history of diabetes. The other patients diagnosed with MIDD (P1–P4) did not have a diagnosis of type II diabetes mellitus (T2DM) as confirmed by normal hemoglobin A1c levels, however, P3 had a family history of diabetes.

All four patients diagnosed with KSS had ptosis and chronic progressive external ophthalmoplegia. Three patients (P6, P7, and P9) presented with a recent history of nyctalopia and either diplopia (P6 and P9) or light sensitivity (P7), whereas P8 had no visual complaints. Three patients (P6, P7, and P8) had a history of cardiac arrhythmias.

### Fundus Imaging

**Maternally Inherited Diabetes and Deafness.** SW-AF images of P1 to P5 demonstrated a speckled appearance within and surrounding the macula (Figs. 1A–E); this feature extended into the periphery in P1 and P3 (see

**TABLE 1.** Clinical and Demographic Summary of Patients Diagnosed With Mitochondrial Disease

| Patient ID/Gender | Ethnicity | Age at Onset/ Evaluation | Diagnosis | BCVA at Evaluation OD, OS | Variant | Biological Sample | Laboratory | Additional Features |
|---|---|---|---|---|---|---|---|---|
| P1–M | Caucasian | 59/61 | MIDD | 20/40, 20/100 | m.3266_3268delAAA | Urine and muscle biopsy | CUMC | Hearing loss, impaired upgaze, mild cerebellar ataxia |
| P2–F | Caucasian | 36/62 | MIDD | 20/25, 20/20 | m.A3243G | Blood | CUMC | Hearing loss |
| P3–F | Caucasian | 44/57 | MIDD | 20/200, 20/25 | m.A3243G | Urine | CUMC | Family history of T2DM |
| P4–M | Caucasian | 53/70 | MIDD | 20/20, 20/20 | m.A3243G | Blood | CUMC | None |
| P5–F | Caucasian | 31/62 | MIDD | 20/60, 20/40 | m.A3243G | Blood | Baylor | Hearing loss, limb weakness, insomnia, depression, T1DM |
| P6–F | Hispanic | 29/33 | KSS | 20/80, 20/50 | m.10246_13616del3371 | Muscle Biopsy | Baylor | Cardiac arrhythmias, T2DM |
| P7–F | Caucasian | 27/28 | KSS | 20/25, 20/25 | Single deletion on Southern blot | Urine | CUMC | Hearing loss, limb weakness, cardiac arrhythmias, nocturnal hypoventilation |
| P8–F | Hispanic | 8/27 | KSS | 20/30, 20/50 | m.G4308A | Muscle Biopsy | CUMC | Cardiac arrhythmias, metabolic syndrome, limb weakness, restless leg syndrome, obstructive sleep apnea |
| P9–M | Caucasian | 28/53 | KSS | 20/20, 20/20 | m.561_3573del3012 | Muscle Biopsy | CUMC | Hearing loss, diplopia, myopathy |

MIDD, maternally inherited diabetes and deafness; KSS, Kearns-Sayre syndrome; N/A, not available; CUMC, Columbia University Medical Center; T2DM, type II diabetes mellitus; T1DM, type I diabetes mellitus; OD, right eye; OS, left eye.

Figs. 1A, 1C). Areas of RPE atrophy were seen in all five patients, with the most significant degeneration occurring in P1, P3, and P5. Only mild patches of parafoveal atrophy were seen in P2. Color fundus photography showed scleral exposure with visualization of the deep choroidal vessels in the area corresponding to the RPE atrophy observed in autofluorescence images (Figs. 2A–E). Vascular attenuation was seen in P1 (see Fig. 2A). The left eyes of P3, P4, and P5 demonstrated the presence of subretinal pigment within the superior temporal arcade, the inferior temporal arcade, and temporal macula region, respectively (see Figs. 2C–E). The subretinal nature of the pigment in P4 and P5 was confirmed using SD-OCT images (see Supplementary Fig. S1). Although SD-OCT images through the pigment were not available for P3, stereoscopic wide field fundus photographs and slit lamp biomicroscopy demonstrated that the pigment was present beneath the retinal vessels.

**Kearns–Sayre Syndrome.** SW-AF images of P6 exhibited widespread RPE atrophy with well-defined scalloped edges. Remaining small patches of retina exhibited a speckled appearance (Fig. 1F). SW-AF images acquired from P7 and P8 displayed a salt-and-pepper appearance surrounding the macula, whereas in P9, this appearance was limited to the far periphery of the retina (Figs. 1G–I). Peripapillary atrophy was seen in all eyes based on SW-AF images and SD-OCT images. Color fundus photography in P6 revealed extensive RPE atrophy with exposure of the deep choroidal vessels and attenuation of the retinal vasculature (Fig. 2F). P7 and P8 presented with mottling of the retina along with vascular attenuation, and optic cupping was seen in P8 (Figs. 2G, 2H). P9 demonstrated RPE changes within the far temporal periphery of the retina (Fig. 2I, dotted inset).

### Combined SD-OCT Findings

SD-OCT images revealed the presence of extensive photoreceptor and RPE atrophy with signal hypertransmission into the choroid in P1 and P3 to P6. SD-OCT images of P2 demonstrated three areas of focal ellipsoid zone (EZ) disruption as well as EZ and RPE loss in the parapapillary region. Images obtained from P7 and P9 revealed intact retinal architecture and RPE, whereas those of P8 displayed some disruption of the interdigitation zone (IZ) with nasal and temporal hypertransmission into the choroid. The fovea was spared in both eyes of P2, P4, P5, P7, P8, and P9 as well as in the left eye of P3 (Figs. 3A–G). Outer retinal tubulations (ORTs) delimited by EZ or external limiting membrane (ELM) that formed the outer borders were observed in both eyes of P3 and P4 (Figs. 4A, 4B). In SW-AF images, foci of faint AF were observed in the atrophic areas and corresponded spatially with the ORTs (see Figs. 4A, 4B, blue arrows). A developing ORT was observed between the central and peripapillary atrophy in the right eye of P2 (see Fig. 4A, yellow arrow). Within areas of complete RPE atrophy, tubulations that did not contain hyper-reflective material were visible (see Fig. 4A, orange arrow). In both eyes of P2, hyper-reflective lesions extending anteriorly through photoreceptor cell-attributable bands were visible; these aberrations corresponded to the hyperautofluorescent flecks seen in SW-AF images (Fig. 4C, blue arrows).

### Electroretinograms

The ffERG results of eight patients (P1, and P3–P9) are summarized in Table 2. P1 and P6 presented with generalized retinal dysfunction with extinguished scotopic responses and residual 30 Hz flicker response with significant implicit time delays. P3, P4, and P7 to P9 presented with normal or diminished 30 Hz flicker amplitudes but no implicit time delay. P5 had decreased cone amplitude and implicit time delay. Scotopic responses were intact in P3, P4, P7, and P9, whereas P5 and P8 had a mild reduction in both scotopic and maximum amplitudes.

### DISCUSSION

Defects of the mitochondria have been implicated in the pathogenesis of numerous retinal degenerations.[1,8–14]
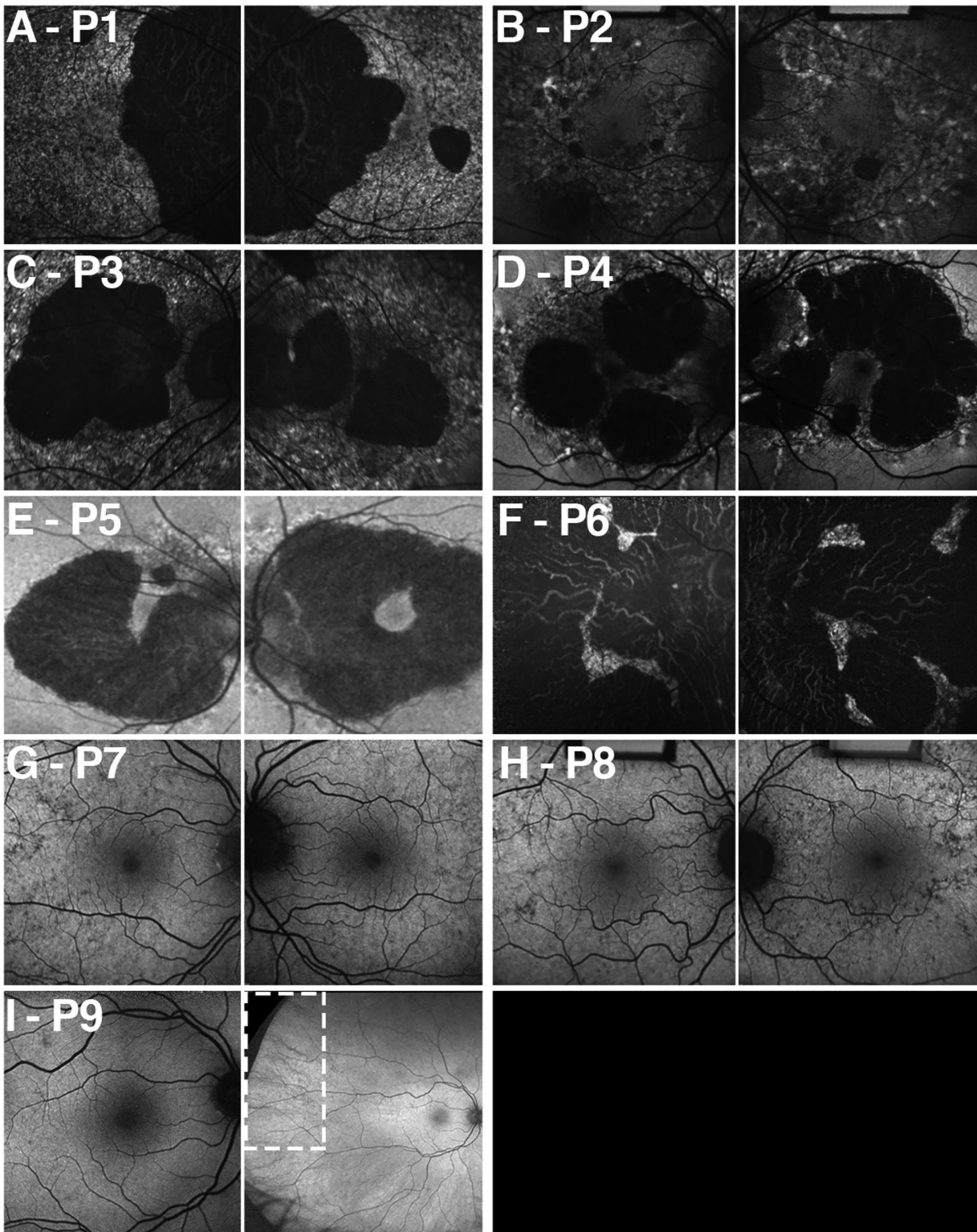
**FIGURE 1.** Short-wavelength autofluorescence images of patients with maternally inherited diabetes and deafness (MIDD) and Kearns-Sayre syndrome (KSS). Short-wavelength autofluorescence imaging demonstrates differing degrees of atrophy of the retinal pigment epithelium in five patients with MIDD (P1–P5, **A–E**) and four with KSS (P6–P9, **F–I**). Extensive atrophy surrounding the optic nerve could be seen in P1, and atrophy within the macula can be seen in P2 to P5. The fovea was spared in 7 of 10 eyes (OU: P2, P4, and P5, OS: P3). An extensive scalloped pattern of atrophy was seen in P6 and a salt-and-pepper pattern of hypoautofluorescence was seen in P7 and P8 **F, G**. Hypoautofluorescence in a fish-net pattern was seen in the periphery of P9 (**H**, dotted inset).
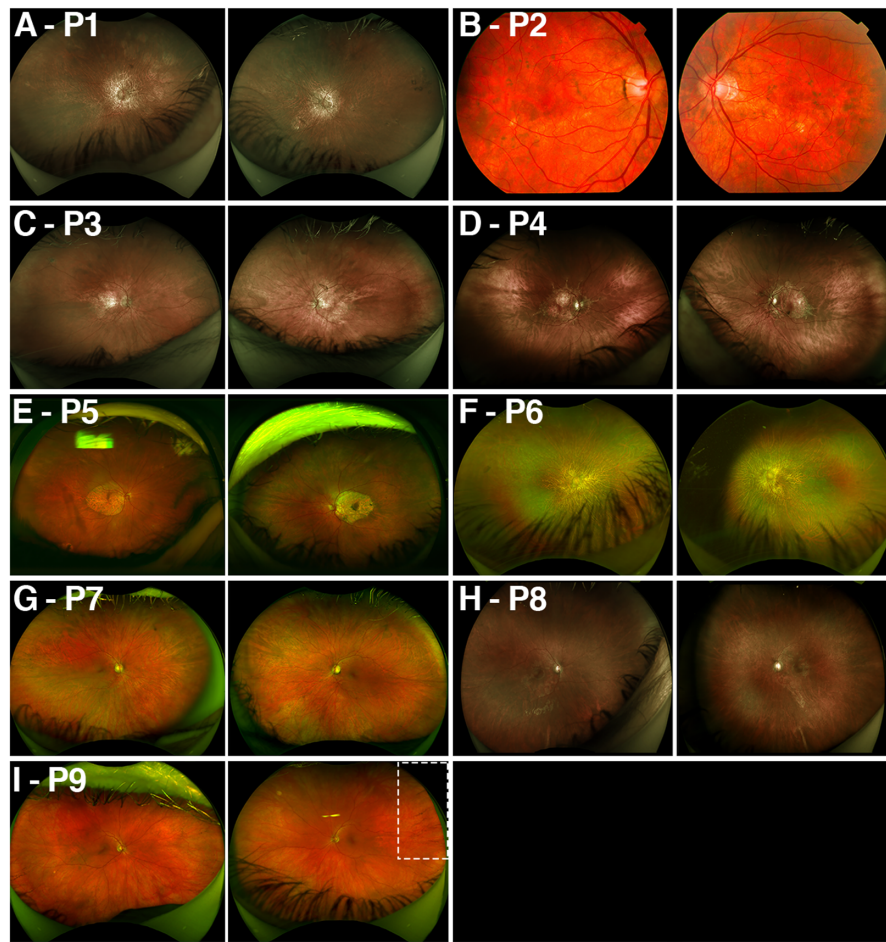
**FIGURE 2.** Color fundus photography in patients with maternally inherited diabetes and deafness (MIDD) and Kearns-Sayre syndrome (KSS). Color fundus photography demonstrates the presence of significant retinal pigment epithelium atrophy in five patients with MIDD (P1–P5, **A–E**). Small subretinal pigment was seen along the superior temporal arcade in the left eye of P3 **C** and superior to the inferior temporal arcade in the left eye of P4 **D**. Significant atrophy was seen in P6 (**F**) with visualization of the deep choroidal vessels and the sclera. A mottling quality was seen within the retinal pigment epithelium of P7 and P8 (**G, H**). Similar mottling was seen in the temporal periphery of P9 (**I**).

**TABLE 2.** Full-Field Electroretinogram Findings of Patients Diagnosed With Mitochondrial Disease

| Patient ID | Scotopic Response OD/OS, µV | Scotopic Response Implicit Time OD/OS, ms | Maximum Response OD/OS A Wave, µV | Maximum Response OD/OS B Wave, µV | Cone Response OD/OS A Wave, µV | Cone Response OD/OS B Wave, µV | 30 Hz Flicker OD/OS, µV | 30 Hz Flicker Implicit Time OD/OS, ms |
|---|---|---|---|---|---|---|---|---|
| P1 | Extinguished | Extinguished | Extinguished | Extinguished | Extinguished | Extinguished | 6.5/7.3 | 39/39 |
| P2 | NA | NA | NA | NA | NA | NA | NA | NA |
| P3 | 98.2/119.2 | 76/94 | −70.9/−83.4 | 168.7/167.1 | −25.2/−16.4 | 108.5/72.4 | 45.5/36.7 | 30/28 |
| P4 | 120.7/219.2 | 73/74 | −143.5/−238.1 | 201/383 | −26.7/−23.9 | 90.7/126.1 | 37.1/75.4 | 28/28 |
| P5 | 181.1/230.8 | 52/52 | −111.1/−117.5 | 171.6/231.5 | −32.4/−19.3 | 74.6/102.7 | 28/50 | 37/37 |
| P6 | Extinguished | Extinguished | Extinguished | Extinguished | Extinguished | Extinguished | 1.1/0.4 | 37/36 |
| P7 | 260.5/212.8 | 96/98 | −149.9/−140.6 | 254.4/270.4 | −13.0/−17.4 | 64.0/34.5 | 43.8/46.9 | 26/31 |
| P8 | 83.7/52.6 | 83/87 | −89.1/−60.6 | 146.6/102.8 | −4.4/−5.4 | 51.0/29.9 | 34.1/29.1 | 28/30 |
| P9 | 130.5/222.6 | 107/89 | −210.8/−266.1 | 342/404.4 | −36.3/−27.7 | 105.4/134.8 | 70.1/98.6 | 32/27 |
| Normal | 218.5 ± 148.3 | 85.9 ± 14.1 | −210.1 ± 172.1 | 347.0 ± 134.1 | −36.4 ± 25.8 | 109.8 ± 67.8 | 121.4 ± 65.5 | 26.3 ± 3.8 |

OD, right eye; OS, left eye; NA, not available.

Mitochondria are known to densely populate both the connecting cilia of photoreceptors, the apical regions of photoreceptor inner segments, as well as the RPE, and given their intimately tied metabolic functions, it is unclear which of these is initially affected.[7] Recent retrospective studies by Müller et al. hypothesized that mitochondrial disease in MIDD may primarily affect the RPE prior to photoreceptors, based on analysis of longitudinal autofluorescence and
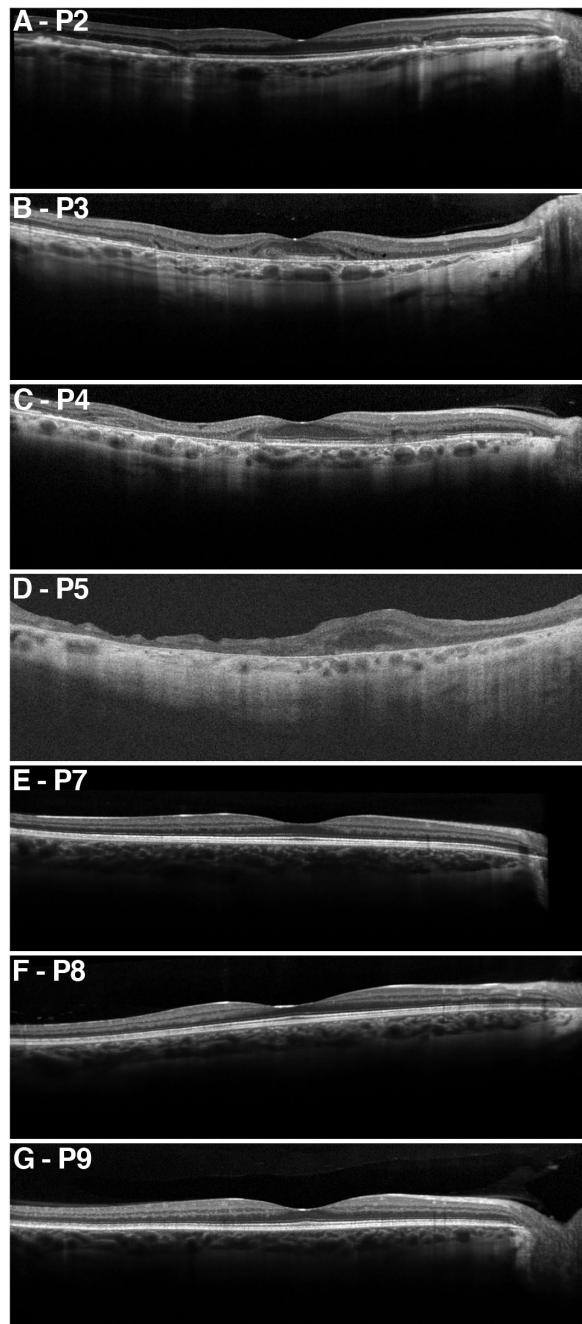
**FIGURE 3.** Foveal sparing in maternally inherited diabetes and deafness (MIDD) and Kearns-Sayre syndrome (KSS). Spectral-domain optical coherence tomography demonstrates foveal sparing in seven eyes of four patients diagnosed with MIDD (P2–P5; **A–D**). The left eye of P3 was flipped and represented here as the right eye **B**. Normal retinal architecture is seen in six eyes of three patients diagnosed with KSS (P7–P9; **E–G**).

SD-OCT findings. Specifically, they found that there was a delay between retinal thinning and visual acuity loss as compared to RPE loss and hypertransmission of OCT signal into the choroid.[19,20] In this study, we expand upon and compare the phenotypic characteristics of a cohort of patients diagnosed with MIDD and KSS and discuss features that may support the hypothesis that initial mitochondrial

dysfunction within the RPE is the primary site of disease pathogenesis.

## Comparison of Disease Phenotypes Between MIDD and KSS

Although MIDD and KSS are both caused by an insult to the mitochondrial genome, retinal and systemic manifestations of disease are dissimilar. Within our cohort, the mean age of visual symptom onset was significantly higher in patients with MIDD (44.6 ± 11.6 years) as compared to patients with KSS (23.0 ± 10.0 years), which was consistent with prior reports in the literature.[19–22] Despite the later onset of disease, the retinal phenotype seen in MIDD was a pattern macular dystrophy with frank RPE atrophy, which was notably more severe than the pigmentary changes and RPE mottling observed in KSS. SD-OCT images in patients with MIDD similarly revealed significant retinal and RPE atrophy with ORTs, whereas those in patients with KSS were unremarkable with the exception of P6. The ffERG was generally spared in both diagnoses, except for in P1 and P6, with minor reductions in 30 Hz flicker amplitudes and no implicit time delay. Visual acuity was well preserved in both conditions, due in part to the foveal sparing characteristic frequently observed in MIDD.

The severity of the retinal phenotype of these two conditions is discordant with the respective sizes of the causative mutation in the mitochondrial genome. Four of five patients diagnosed with MIDD carried the common m.A3243G point mutation and one patient (P1) possessed a novel 3 base pair (bp) deletion within 25 bp of the classic mutation. In contrast, although specific deletions were only identified in two of the four patients diagnosed with KSS, the deletions spanned over 3000 bp in both cases. Interestingly, the deletion identified in P9, m.561_3573del3012, also leads to the loss of *MT-TL1*; however, the retinal phenotype in this patient did not resemble MIDD and was similar to the other cases of KSS. A possible explanation for this disparity may lie in the difference in mutation heteroplasmy within the neurosensory retina. In other words, there may be a higher prevalence of MIDD-associated mutations in *MT-TL1* than KSS-related large-scale deletions in the mitochondria of retina cells.

A recently published autofluorescence study of MIDD observed that retinal degeneration developed at eccentricities of 10 to 20 degrees with foveal sparing, unlike in other macular dystrophies, which typically affect the center.[19] This feature was also observed in our patients, although the fovea was affected in both eyes of P1 and the right eye of P3. We hypothesize that this parafoveal atrophy and foveal sparing may in part be due to a higher heteroplasmy levels of the mutation specifically in the cells at eccentricities of 10 degrees to 20 degrees as compared to the rest of the retina, or due to the varied expression of antioxidant enzymes described in proteomic analyses of these anatomic regions in the RPE and retina.[23,24] In the setting of the salt-and-pepper retinopathy seen in KSS in an otherwise normal retina, we hypothesize that the hypo-autofluorescent spots seen on SW-AF and the areas of mottling seen on fundus photography may coincide with clusters of cells with higher heteroplasmy rates for these large deletions. Further studies, such as histopathology, adaptive optics, and additional proteomic analyses, are warranted to corroborate these hypotheses.
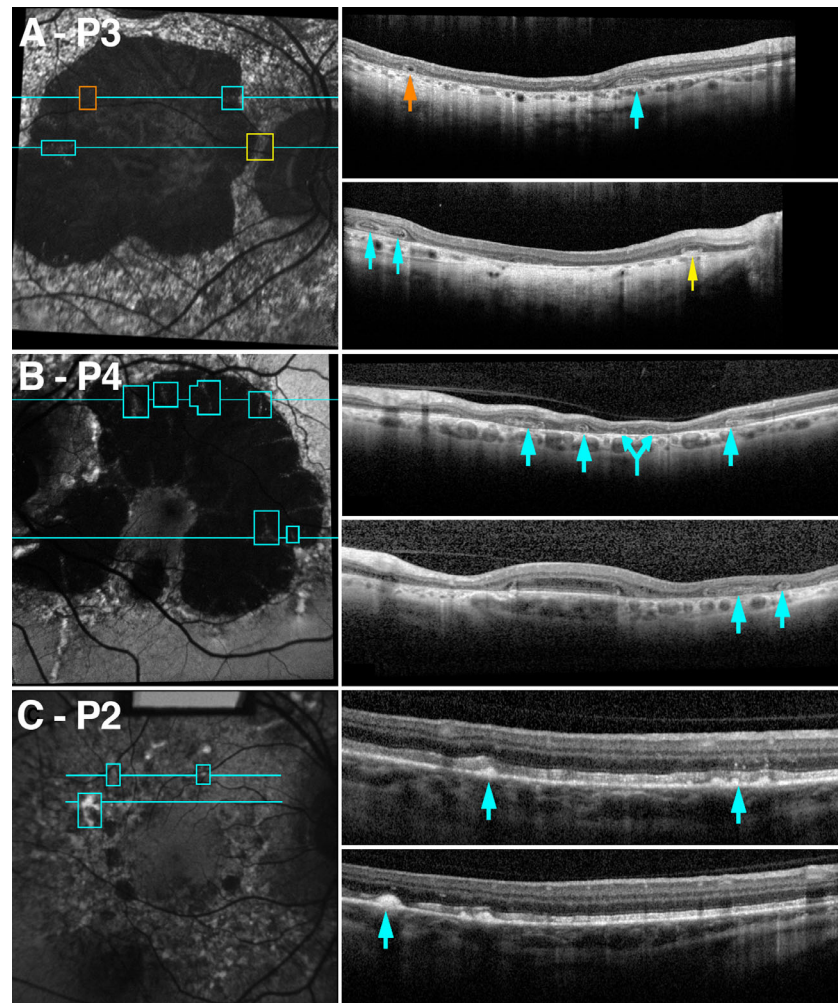
**Figure 4.** Correspondence of outer retinal tubulations with autofluorescence speckling in maternally inherited diabetes and deafness (MIDD). Spectral-domain optical coherence tomography and short-wavelength autofluorescence imaging is shown for three patients (P2, P3, and P4) diagnosed with MIDD (**A–C**). Autofluorescence revealed that the faint foci of AF **A** and **B** (cyan boxes) seen along the borders of retinal pigment epithelial atrophy correlated spatially with the presence of outer retinal tubulations (ORTs) on optical coherence tomography **A** and **B** (cyan arrows). A nascent ORT **A** (yellow arrow) was identified in the speckled hyperautofluorescent region between the central RPE atrophy and peripapillary atrophy, which may be suggestive of impending atrophy in this location. These peripheral ORTs contained hyper-reflective foci **A** and **B** (cyan arrows) that are trapped within these tubulations. In tubulations located deeper within the atrophy on fundus autofluorescence, no hyper-reflective foci were seen **A** (orange arrow). In P2, hyper-reflective lesions (**C**, cyan arrows) were present, which correlated spatially with foci of hyperautofluorescence **C** (cyan boxes).

In addition to the notable differences between retinal manifestations of MIDD and KSS, unusual phenotypes were observed even within each respective group. Notably, P1 presented with an unusual phenotype for MIDD that more significantly affected the peripapillary region as compared to the macula, with islands of atrophy extending nasally and superiorly to the disc. Similarly, P6, who was found to have a large 3371 bp deletion, presented with a choroideremia-like phenotype that was dissimilar to the classic KSS phenotype seen in the other patients. The difference in the phenotype of P1 to the other patients with MIDD may be attributable to the novel mutation, which causes a deletion as opposed to the single point mutation commonly implicated in MIDD.[22] The cause of the unusual phenotype observed in P6 is unclear, and has only been reported once before in the literature.[25] Notably, the reported case was described in 1993 when genetic testing capabilities were limited.[25] Consequently, we hypothesize this phenotype may be caused by either

a potentially confounding genetic modifier or an unusually high rate of mutation heteroplasmy in the retina. P1 underwent additional genetic screening with a subsequent negative whole exome sequence; however, P6 declined to undergo further genetic testing.

## Additional Features Suggestive of Primary RPE Disease

In recent studies of MIDD, Müller et al. have hypothesized that RPE atrophy may precede photoreceptor death in MIDD, and by extension mitochondrial diseases, based upon a combination of longitudinal SW-AF and SD-OCT analysis, which revealed a delay between RPE atrophy and subsequent visual acuity loss and retinal thinning as seen on SD-OCT.[19,20] In our cohort, we observed a number of additional features that support this hypothesis in both MIDD and KSS.

**Maternally Inherited Diabetes and Deafness.** Stereoscopic view through a slit lamp biomicroscope and color fundus photography of the patients with MIDD suggest evidence for primary RPE disease based upon the absence of intraretinal pigment migration. Intraretinal pigment migration is a classic feature of several degenerative photoreceptor disorders, such as retinitis pigmentosa, and occurs as a result of RPE cells that migrate into the retina following the loss of apposition to photoreceptor cells.[26–28] Takahashi et al. suggested that it takes an average of 5.4 years for intraretinal pigment migration to appear in patients with retinitis pigmentosa sine pigmento.[29] However, the age range of patients in that study who developed new intraretinal pigment was between 7 and 37 years of age. Older patients who did not present with intraretinal pigment migration did not develop the phenotype. All 5 patients diagnosed with MIDD were significantly older, with a median age of 62 years at presentation.

In a recent study of intraretinal pigment migration across inherited retinal dystrophies, we found that pigment migration is rarer in patients with disease caused by mutations in genes specific to the RPE (34.0%) as compared to patients with mutations in genes specific to the photoreceptors (75.8%).[30] The absence of pigment in disease due to mutations in RPE-specific genes becomes even more pronounced (6.9%) when cases of choroideremia, a disease in which photoreceptors and RPE have been suggested to degenerate independently, were excluded.[30] Mutations in RPE-specific genes were hypothesized to lead to primary RPE degeneration prior to photoreceptor loss, thereby preventing pigment migration. Although the absence of pigment is not a specific finding of mutations in RPE-specific genes, in all five patients with MIDD, we observed the absence of intraretinal pigment migration, which may suggest that mutations in *MT-TL1* also lead to primary degeneration of the RPE. This is further supported by our understanding of the physiological function of *MT-TL1*, which serves as a key building block in the components of the oxidative phosphorylation chain, the primary source of energy for the RPE but not the photoreceptors.[2–7,31,32]

An examination of the areas of RPE atrophy as well as the surrounding macula demonstrated a correlation between ORTs seen on SD-OCT and the faint foci of autofluorescence (AF) presenting as invaginations within the islands of atrophy on SW-AF (see Figs. 4A, 4B, blue boxes). This spatial correlation of newly developing ORTs occurring at the boundary of preserved and atrophic RPE as seen on SW-AF has been previously described by Goldberg et al. who suggest these areas may retain residual function, as well as by Müller et al. in their recent study.[19,33] In an area of intact retina located between two separate islands of atrophy, the presence of a developing ORT was observed, which may predict impending RPE atrophy at this location (see Fig. 4A, yellow arrow). This is consistent with the observation by Müller et al. who suggested that coalescing outer retinal atrophy gave rise to ORTs.[20] In both P3 and P4 as well as in previously reported cases, the ORTs occurring at the boundary of intact and atrophic RPE were found to contain hyper-reflective debris (see Fig. 4, blue arrows). This hyper-reflectance was absent from ORTs located deeper within the areas of RPE atrophy (see Fig. 4A, orange arrow).[33,34] Based on this observation, we hypothesize that these faint foci of AF on SW-AF imaging may originate from the presence of bisretinoids within the photoreceptor outer segments enclosed by the ORTs. Bisretinoids

within the RPE are frequently mistaken to be the only source of AF; however, AF originating from photoreceptor cells have been demonstrated in patients with retinitis pigmentosa as well as in fundus flecks associated with recessive Stargardt disease.[35,36] Additionally, AF emitted from the interior of photoreceptor rosettes, which are believed to be the murine equivalent of ORTs, in mouse models of retinal degeneration has been described.[37] The absence of these hyper-reflective foci in SD-OCT scans at points deeper within the atrophic regions suggests that over time these photoreceptor remnants are lost completely.

ORTs are a recently described feature of degenerative retinal diseases and are believed to form in the setting of RPE or choroidal death.[38,39] Prior studies have proposed that the development of ORTs occurs as the result of insult to photoreceptors, likely secondary to RPE damage or loss of interdigitation of the photoreceptors with the RPE, after which activated Müller cells descend, expand, and surround the remnants of damaged photoreceptors to form longitudinal tubulations.[34,38] ORTs can be identified not only in advanced AMD, but also pattern macular dystrophies, choroideremia, gyrate atrophy, and Bietti crystalline dystrophy.[33,38,40] Notably, the pathophysiology of each of the described conditions with ORTs has been hypothesized to involve primary RPE degeneration.[41–47]

**Kearns–Sayre Syndrome.** Unlike the progression observed in the retinal phenotype of MIDD, the retinal degeneration associated with KSS is significantly milder and more stable. Consequently, the evidence for primary dysfunction at the level of the RPE is more difficult to prove. The characteristic feature observed in this cohort of patients with KSS was the presence of hypo-autofluorescent spots on SW-AF and mottling as seen on color fundus photography that is classically described as a salt-and-pepper retinopathy. Such pigmentary changes bear a striking resemblance to other disorders, such as rubella retinopathy and choroideremia carriers, that can present with a salt-and-pepper fundus appearance.[48–50] In rubella retinopathy, the pigmentary changes have been reported to occur in the setting of focal atrophy and pigmentary changes in the RPE with sparing of the retina and choroid.[48,49]

Choroideremia carriers specifically present an interesting parallel to patients with KSS and may provide further insight into the pathophysiology of KSS. Whether the primary site of degeneration in choroideremia is the RPE or the photoreceptors is still unclear, it is understood that the mottling pigmentary changes seen in choroideremia carriers occurs as a result of lyonization, or the random inactivation of the X-chromosome in certain cells but not others.[50,51] Mottled or affected areas, which appear hypo-autofluorescent on SW-AF, would coincide with areas where the mutant X-chromosome is highly expressed.[40,50] This bears some similarity to the importance of heteroplasmy in mitochondrial degenerations and how it may affect phenotypic appearance. Consequently, we may hypothesize that the characteristic appearance of KSS may be due to differences in heteroplasmy across the retina.

Overall, these observations link the pathogenesis of primary mitochondrial disorders to the RPE, and parallels can be drawn to other retinal diseases, such as AMD. Notable similarities between the features of the two disorders exist, with the presence of outer retinal tubulations and subretinal deposits, prominent RPE atrophy, and spared ffERG in the absence of global retinal disease.[52–55] The accumulation of damaged mtDNA in patients with AMD has been shown to

contribute to disease pathogenesis and several studies have suggested that mitochondrial loss within the RPE is one of the critical pathogenic events in AMD.[7–11] Notably, Terluk et al. showed that several genes are associated with increased damage in patients with AMD, including *MT-TL1*, the gene encoding for tRNA leucine.[9] This gene is implicated in over 80% of cases of MIDD and is involved in 5 patients in this cohort.[55] Similarly, the majority of cases of KSS involve major deletions that span the mitochondrial genome.[56,57]

### Limitations and Future Directions

Although we describe a number of phenotypic similarities between primary mitochondrial degenerations and conditions that are believed to involve primary RPE degeneration, there are a number of limitations to this study. The retrospective and cross-sectional approach of analysis in this study make it difficult to assess temporal changes to retinal structure. Consequently, although we hypothesize that the RPE was affected first, we cannot determine with certainty that this is the case. Furthermore, the inferences of our study are limited by a relatively small sample size. A recent longitudinal analysis of SD-OCT images in MIDD included a total of three eyes without RPE or outer retinal atrophy at initial presentation.[20] The study suggested that dysfunction first presented as EZ loss and subretinal deposits followed afterwards by RPE degeneration and hypertransmission into the choroid.[20] Evaluation of a larger cohort of patients who are early on in the disease process will help corroborate these findings. Notably, the SD-OCT images of P2 revealed subretinal deposits and relatively spared EZ; consequently, long-term follow-up of this patient will be valuable. Alternative mechanisms may include a concurrent or staggered degeneration of the RPE and photoreceptors, similar to a mechanism that has been previously described in choroideremia.[58] Longitudinal prospective studies will help define more exact mechanisms.

The elucidation of clearer pathophysiological steps and the mechanism of primary mitochondrial diseases may improve our understanding of retinal disorders that are known to involve secondary mitochondrial degeneration, such as AMD. Nonetheless, the application of this understanding to secondary mitochondrial degenerations may be limited due to the multifactorial and complex nature of such disorders. Analysis of a larger sample of patients with primary mitochondrial diseases coupled with mechanistic studies would be required to validate our hypothesis that the degeneration of the RPE is the primary pathophysiological step in these conditions and is due to mitochondrial dysfunction within the RPE.

### Acknowledgments

Disclosure: **J.K. Oh**, None; **J.R. Lima de Carvalho Jr**, None; **Y. Nuzbrokh**, None; **J. Ryu**, None; **T. Chemudupati**, None; **V.B. Mahajan**, None; **J.R. Sparrow**, None; **S.H. Tsang**, None

### *References*

1. Lefevere E, Toft-Kehler AK, Vohra R, Kolko M, Moons L, Van Hove I. Mitochondrial dysfunction underlying outer retinal diseases. *Mitochondrion*. 2017;36:66–76.

2. Kanow MA, Giarmarco MM, Jankowski CS, et al. Biochemical adaptations of the retina and retinal pigment epithelium support a metabolic ecosystem in the vertebrate eye. *eLife*. 2017;6:e28899.

3. Du J, Rountree A, Cleghorn WM, et al. Phototransduction influences metabolic flux and nucleotide metabolism in mouse retina. *J Biol Chem*. 2016a;291:4698–4710.

4. Chinchore Y, Begaj T, Wu D, Drokhlyansky E, Cepko CL. Glycolytic reliance promotes anabolism in photoreceptors. *eLife*. 2017;6:e25946.

5. Hurley JB, Lindsay KJ, Du J, Glucose DJ. Glucose, lactate, and shuttling of metabolites in vertebrate retinas. *J Neurosci Res*. 2015;93:1079–1092.

6. Winkler BS. Glycolytic and oxidative metabolism in relation to retinal function. *J Gen Physiol*. 1981;77:667–692.

7. Medrano CJ, Fox DA. Oxygen consumption in the rat outer and inner retina: light- and pharmacologically-induced inhibition. *Exp Eye Res*. 1995;61:273–284.

8. Fisher CR, Ferrington DA. Perspective on AMD pathobiology: a bioenergetic crisis in the RPE. *Invest Ophthalmol Vis Sci*. 2018;59:AMD41–AMD47.

9. Terluk MR, Kapphahn RJ, Soukup LM, et al. Investigating mitochondria as a target for treating age-related macular degeneration. *J Neurosci*. 2015;35:7304–7311.

10. Ferrington DA, Fisher CR, Kowluru RA. Mitochondrial defects drive degenerative retinal diseases. *Trends Mol Med*. 2020;26:105–118.

11. Feher J, Kovacs I, Artico M, Cavallotti C, Papale A, Balacco Gabrieli C. Mitochondrial alterations of retinal pigment epithelium in age-related macular degeneration. *Neurobiol Aging*. 2006;27:983–993.

12. Ferrington DA, Kapphahn RJ, Leary MM, et al. Increased retinal mtDNA damage in the CFH variant associated with age-related macular degeneration. *Exp Eye Res*. 2016;145:269–277.

13. Brennan LA, Kantorow M. Mitochondrial function and redox control in the aging eye: role of MsrA and other repair systems in cataract and macular degenerations. *Exp Eye Res*. 2009;88:195–203.

14. Karunadharma PP, Nordgaard CL, Olsen TW, Ferrington DA. Mitochondrial DNA damage as a potential mechanism for age-related macular degeneration. *Invest Ophthalmol Vis Sci*. 2010;52:5470.

15. Fritsche LG, Igl W, Bailey JN, et al. A large genome-wide association study of age-related macular degeneration highlights contributions of rare and common variants. *Nat Genet*. 2016;48:134–143.

16. Ratnapriya R, Chew EY. Age-related macular degeneration-clinical review and genetics update. *Clin Genet*. 2013;84:160–166.

17. Ferrington DA, Kapphahn RJ, Leary MM, et al. Increased retinal mtDNA damage in the CFH variant associated with

age-related macular degeneration. *Exp Eye Res.* 2016;145:269–277.

18. Marmor MF, Fulton AB, Holder GE, et al. ISCEV Standard for full-field clinical electroretinography (2008 update). *Doc Ophthalmol.* 2009;118:69–77.

19. Müller PL, Treis T, Pfau M, et al. Progression of retinopathy secondary to maternally inherited diabetes and deafness–evaluation of predicting parameters. *Am J Ophthalmol.* 2020;213:134–144.

20. Müller PL, Maloca P, Webster A, Egan C, Tufail A. structural features associated with the development and progression of rora secondary to maternally inherited diabetes and deafness. *Am J Ophthalmol.* 2020;218:136–147.

21. Mancuso M, Orsucci D, Angelini C, et al. Redefining phenotypes associated with mitochondrial DNA single deletion. *J Neurol.* 2015;262:1301–1309.

22. Michaelides M, Jenkins SA, Bamiou DE, et al. Macular dystrophy associated with the A3243G mitochondrial DNA mutation. Distinct retinal and associated features, disease variability, and characterization of asymptomatic family members. *Arch Ophthalmol.* 2008;126:320–328.

23. Skeie JM, Mahajan VB. Proteomic landscape of the human choroid-retinal pigment epithelial complex. *JAMA Ophthalmol.* 2014;132:1271–1281.

24. Velez G, Machlab DA, Tang PH, et al. Proteomic analysis of the human retina reveals region-specific susceptibilities to metabolic- and oxidative stress-related diseases. *PLoS One.* 2018;13:e0193250.

25. Herzberg NH, van Schooneveld MJ, Bleeker-Wagemakers EM, et al. Kearns-Sayre syndrome with a phenocopy of choroideremia instead of pigmentary retinopathy. *Neurology.* 1993;43:218–221.

26. Li ZY, Possin DE, Milam AH. Histopathology of bone spicule pigmentation in retinitis pigmentosa. *Ophthalmology.* 1995;102:805–816.

27. Milam AH, Li ZY, Fariss RN. Histopathology of the human retina in retinitis pigmentosa. *Prog Retin Eye Res.* 1998;17:175–205.

28. Kim JW, Kang KH, Burrola P, Mak TW, Lemke G. Retinal degeneration triggered by inactivation of PTEN in the retinal pigment epithelium. *Genes Dev.* 2008;22:3147–3157.

29. Takahashi VKL, Takiuti JT, Jauregui R, Mahajan VB, Tsang SH. Rates of bone spicule pigment appearance in patients with retinitis pigmentosa sine pigmento. *Am J Ophthalmol.* 2018;195:176–180.

30. Oh JK, Levi SR, Kim J, et al. Differences in intraretinal pigment migration across inherited retinal dystrophies [published online ahead of print, 2020 May 19]. *Am J Ophthalmol,* https://doi.org/10.1016/j.ajo.2020.05.010.

31. Sasarman F, Antonicka H, Shoubridge EA. The A3243G tRNALeu(UUR) MELAS mutation causes amino acid misincorporation and a combined respiratory chain assembly defect partially suppressed by overexpression of EFTu and EFG2. *Hum Mol Genet.* 2008;17:3697–3707.

32. Fornuskova D, Brantova O, Tesarova M, et al. The impact of mitochondrial tRNA mutations on the amount of ATP synthase differs in the brain compared to other tissues. *Biochim Biophys Acta.* 2008;1782:317–325.

33. Goldberg NR, Greenberg JP, Laud K, Tsang S, Freund KB. Outer retinal tubulation in degenerative retinal disorders. *Retina.* 2013;33:1871–1876.

34. Dolz-Marco R, Litts KM, Tan ACS, Freund KB, Curcio CA. The evolution of outer retinal tubulation, a neurodegeneration and gliosis prominent in macular diseases. *Ophthalmology.* 2017;124:1353–1367.

35. Schuerch K, Woods RL, Lee W, et al. Quantifying fundus autofluorescence in patients with retinitis pigmentosa. *Invest Ophthalmol Vis Sci.* 2017;58:1843–1855.

36. Paavo M, Lee W, Allikmets R, Tsang S, Sparrow JR. Photoreceptor cells as a source of fundus autofluorescence in recessive Stargardt disease. *J Neurosci Res.* 2019;97:98–106.

37. Flynn E, Ueda K, Auran E, Sullivan JM, Sparrow JR. Fundus autofluorescence and photoreceptor cell rosettes in mouse models. *Invest Ophthalmol Vis Sci.* 2014;55:5643–5652.

38. Zweifel SA, Engelbert M, Laud K, Margolis R, Spaide RF, Freund KB. Outer retinal tubulation: a novel optical coherence tomography finding. *Arch Ophthalmol.* 2009;127:1596–1602.

39. Schaal KB, Freund KB, Litts KM, Zhang Y, Messinger JD, Curcio CA. Outer retinal tubulation in advanced age-related macular degeneration: optical coherence tomographic findings correspond to histology. *Retina.* 2015;35:1339–1350.

40. Paavo M, Jr Carvalho JRL, Lee W, Sengillo JD, Tsang SH, Sparrow JR. Patterns and intensities of near-infrared and short-wavelength fundus autofluorescence in choroideremia probands and carriers. *Invest Ophthalmol Vis Sci.* 2019; 60:3752–3761.

41. Syed R, Sundquist SM, Ratnam K, et al. High-resolution images of retinal structure in patients with choroideremia. *Invest Ophthalmol Vis Sci.* 2013;54:950–961.

42. Oh KT. Pattern Dystrophies of the RPE. In: Traboulsi EI, Traboulsi EI . *Genetic diseases of the eye.* 2nd ed. New York: Oxford University Press; 2012.

43. MacDonald IM, Russell L, Chan CC. Choroideremia: new findings from ocular pathology and review of recent literature. *Surv Ophthalmol.* 2009;54:401–407.

44. Flannery JG, Bird AC, Farber DB, et al. A histopathologic study of a choroideremia carrier. *Invest Ophthalmol Vis Sci.* 1990;31:229–236.

45. Wang T, Milam AH, Steel G, Valle D. A mouse model of gyrate atrophy of the choroid and retina. Early retinal pigment epithelium damage and progressive retinal degeneration. *J Clin Invest.* 1996;97:2753–2762.

46. Wilson DJ, Weleber RG, Klein ML, Welch RB, Green WR. Bietti's crystalline dystrophy. A clinicopathologic correlative study. *Arch Ophthalmol.* 1989;107:213–221.

47. Halford S, Liew G, Mackay DS, et al. Detailed phenotypic and genotypic characterization of Bietti crystalline dystrophy. *Ophthalmology.* 2014;121:1174–1184.

48. Duszak RS. Congenital rubella syndrome–major review. *Optometry.* 2009;80:36–43.

49. Arnold JJ, McIntosh ED, Martin FJ, Menser MA. A fifty-year follow-up of ocular defects in congenital rubella: late ocular manifestations. *Aust N Z J Ophthalmol.* 1994;22:1–6.

50. Bonilha VL, Trzupek KM, Li Y, et al. Choroideremia: analysis of the retina from a female symptomatic carrier. *Ophthalmic Genet.* 2008;29:99–110.

51. Lyon MF. Gene action in the X-chromosome of the mouse (Mus musculus L.). *Nature.* 1961;190:372–373.

52. Litts KM, Messinger JD, Dellatorre K, Yannuzzi LA, Freund KB, Curcio CA. Clinicopathological correlation of outer retinal tubulation in age-related macular degeneration. *JAMA Ophthalmol.* 2015;133:609–612.

53. Gerth C. The role of the ERG in the diagnosis and treatment of age-related macular degeneration. *Doc Ophthalmol.* 2009;118:63–68.

54. Hogg RE, Chakravarthy U. Visual function and dysfunction in early and late age-related maculopathy. *Prog Retin Eye Res.* 2006;25:249–276.

55. Naing A, Kenchaiah M, Krishnan B, et al. Maternally inherited diabetes and deafness (MIDD): diagnosis and management. *J Diabetes Complications.* 2014;28:542–546.

56. Saldana-Martinez A, Munoz ML, Perez-Ramirez G, et al. Whole sequence of the mitochondrial DNA genome of

Kearns Sayre Syndrome patients: Identification of deletions and variants. *Gene*. 2019;688:171–181.

57. Remes AM, Majamaa-Voltti K, Kärppä M, et al. Prevalence of large-scale mitochondrial DNA deletions in an adult Finnish population. *Neurology* 2005;64:976–81.

58. Tolmachova T, Anders R, Abrink M, et al. Independent degeneration of photoreceptors and retinal pigment epithelium in conditional knockout mouse models of choroideremia. *J Clin Invest*. 2006;116:386–394.